TONELLI PRINCIPLE: FINITE REDUCTION AND FIXED ENERGY MOLECULAR DYNAMICS TRAJECTORIES

A. TURCO[†], D. PASSERONE[‡], AND F. CARDIN[§]

Abstract. We propose a novel theoretical and practical alternative to the Maupertuis functional in the field of molecular dynamics: Tonelli functional. Our aim is to adapt this technique to the study of rare events where the initial and the final state of a system are known and we look for transition paths. We reached it with a rigorous mathematical development of the functional and an efficient numerical algorithm. We couple the Tonelli functional with an exact finite dimensional reduction and we prove error estimates for its implementation. This is not far from a multiscale approach, indeed the reduction will help the study of the high frequencies of the systems: it can be seen as a magnifying glass for atomic trajectories. We test our techniques first on simple models, in order to show the details and the main features of these new tools: an harmonic oscillator, a one dimensional double-well potential, the well tested Mueller potential and a short oscillatory trajectory of a 4 atom cluster are studied under different points of view. Then we pass to a more demanding test: the isomerization of a Lennard-Jones cluster of 38 interacting atoms.

Key words. Lagrangian Mechanics, Calculus of Variations, Molecular dynamics, Rare events.

AMS subject classifications. 49S05, 65K10, 65P10, 70G75, 70H30

1. Introduction. The variational principles of classical mechanics govern the existence and the characterization of dynamical trajectories connecting two points in configuration or phase space. Such dynamical trajectories joining two fixed points can show different regimes according the the underlying potential energy profile. Let us think, for example, of a rare transition event overcoming a barrier between two stable states with a total energy just above the energy of the transition state. The trajectory describing such event will have regions with fast oscillations close to the reactant and the product basins, and a region close to the transition state with well known temporal instabilities.

In this paper we propose two techniques which can improve the understanding of the problem. On one hand we introduce Tonelli principle that allows us to describe properly situations in which the total energy is close to the potential energy. On the other hand we discuss a finite reduction scheme that leads to a computationally convenient strategy for treating the different timescales of the trajectory.

Tonelli functional is a variational formulation of the Lagrange equations whose name is devoted to the mathematician who first proposed it [1]. More recently it was used by A. Ambrosetti [2] and G. F. Dell'Antonio [3] to find periodic solutions for Hamiltonian systems. In section §2 we present a modification of their setting in which the trajectories have fixed end points. The first peculiarity of this tool (in a way similar, but not equal, to what the Maupertuis functional does) is that we need not to specify the time in which the system has to pass from the initial (q_0) to the final (q_1) state: given the energy E the functional selects the right time and gives a simple (i.e. linear) relation to obtain the mechanical parametrization of the path from the geometric one. Moreover in this way we overcome the singularity appearing in the time reparametrization of Maupertuis principle at the vanishing velocity points.

[†]Scuola Internazionale Superiore di Studi Avanzati, Via Beirut 2, 34014 Trieste, Italy

[‡]EMPA - Swiss Federal Laboratories for Materials Testing and Research, Uberlandstr. 129, 8600 Duebendorf, Switzerland

[§]Dipartimento di Matematica Pura ed Applicata, Università degli Studi di Padova, via Trieste 63, 35121 Padova, Italy

A further step toward the numerical implementation is done in section §3, where we prove an exact finite dimensional reduction. Similar techniques have been proposed by Amann, Conley and Zehnder [4, 5] with the aim to transform a variational problem (over an infinite dimensional space of curves) into an algebraic one. Here we focus on a possible application to the search of stationary points of Tonelli functional. Exploiting the advantages of both Tonelli and the reduction technique we can optimize the computational efforts and concentrate them on a lower number of unknowns and nevertheless we obtain detailed trajectories.

In section §4 we enter in the details of the numerical algorithm; we first show the differences between Tonelli functional and Maupertuis one. We tested them on a simple case, where the number of degrees of freedom are not too many and we can directly find the stationary points (without using the reduction). Tonelli guarantees higher precision, as we show with a one dimensional double-well potential, and can efficiently explore trajectory space, as we show with the well-known Mueller potential. Then, in section §5, we explain how the key point of the reduction technique, a contractive iterative map, can be translated in a numerical tool. We present also some estimates on the error we can make following this method and we prove that this error (if some parameters are well tuned) is of the same order of magnitude than the one we can expect from a typical path discretization.

The algorithm and the mathematics behind it can be hard to understand at a first glance. This is why we add a simple test case, before testing our strategy on more demanding systems. In section §6 we show step by step the implementation of the technique on a oscillatory trajectory of a cluster of 4 atoms of argon. Clearly what is important here is not the physics we observe, this example is useful for the comprehension of the previous sections and also of the last subsection, where we finally work on a physically interesting case. We chose for that a typical benchmark in Molecular Dynamics, the isomerization of a 38 atom cluster, interacting through a Lennard-Jones potential.

The problem of how to treat the different timescales in a dynamical trajectory has been faced by several authors [10, 11, 12, 13, 14, 15]. Before entering in the details, we want to explain why the computation of a single trajectory is interesting also from the point of view of path sampling. As pointed out in previous studies (see, e.g., Bai and Elber [16] and references therein) two-point boundary algorithms applied to a description where all microscopic degrees of freedom are considered explicitly can become exceedingly expensive when the total time of the path becomes too large. Nevertheless, Bai and Elber point out that short time trajectories can become statistically important if one focuses on the transitional part of a reactive path from a reactant to a product. If the process is not diffusive, the very transition process is rather short, and a sampling limited to the transition part of the path can give informations on the transient timescale of the process. It is in this kind of processes that two-point boundary algorithms can play their role.

In this paper, we will not discuss at all sampling. Instead, we will propose a new method for obtaining accurate trajectories at a fixed energy, a feature that could be used for subsequent extensions of sampling strategies. The first direct application could be envisioned in the microcanonical sampling with a modified Boltzmann criterion in order to enhance the sampling of important energy regions with low density of states (Wang-Landau method [17]). Another extension could be the field of extended Lagrangians (for example for systems in contact with a thermostat), where an extended conserved quantity (total "energy") can be defined for the whole system

(e.g., solute + solvent + thermostat), and a controlled sampling as a function of this quantity could be introduced.

However, the introduction of a novel variational principle (although already well known in the field of differential geometry and classical mechanics of periodic orbits) into the realm of complex multidimensional systems is useful *per se*. If, as we hope to have achieved, a correspondent computational strategy for obtaining accurate paths is developed, then we have a new tool for understanding the microscopic mechanisms underlying a physical or chemical process.

2. Tonelli Principle. Classical variational principles - Hamilton, Hamilton-Helmholtz, Maupertuis among others - are the tools of choice when one looks for a trajectory with fixed end points. For trajectories at prescribed energy the most popular principle is the one due to Maupertuis. Tonelli principle [1], introduced in the present paper in a novel context, works in the same spirit but exhibits some different and interesting features. We consider an $\mathcal{N}$-body problem and we define a reference time interval $(0,1)$ (the physical correct time will be restored at the end of the procedure) on which we can define the space of admissible trajectories as:

$$\Gamma_{q_0,q_1} = \left\{ q(\cdot) \in H^1((0,1),\mathbb{R}^{3\mathcal{N}}) : \quad q(0) = q_0, \quad q(1) = q_1 \right\}. \tag{2.1}$$

The functional space H^1 is mandatory for this technique, but at the end we will recover classical curves with well defined velocities and accelerations. For the moment we recall that by $H^k\left((0,1),\mathbb{R}^{3\mathcal{N}}\right)$ we mean the space of the curves that lie in L^2 together with their derivatives up to order k. For any fixed real value h (that will be the total energy of the system), Tonelli functional is

$$\mathcal{T}_h(q(\cdot)) = \int_0^1 K(\dot{q}(\tau))\, d\tau \cdot \int_0^1 (h - V(q(\tau)))\, d\tau \tag{2.2}$$

where $K(\dot{q}) = \frac{1}{2}\sum_{i=1,\dots,\mathcal{N}\,\alpha=1,2,3} m_i(\dot{q}^i_\alpha)^2$ is the kinetic energy and $V(q)$ is the potential energy function. This potential can be singular, as the classical Lennard-Jones which prevents any possible collision giving them an infinite energy, remaining on the other hand bounded from below. In order to perform the regularity theory on the solution of the problem, we require the potential to be smooth under the value of the total energy that we will fix. For the sake of simplicity, we have chosen masses $m_i \equiv 1,\ i = 1,\dots,\mathcal{N}$.

The mathematical formulation of Tonelli principle goes as follows. Suppose that $q(\cdot)$ is an admissible curve such that $\mathcal{T}_h(q) > 0$, and consider also a reparametrization of the form:

$$[0,\omega^{-1}] \ni t \mapsto \bar{q}(t) := q(t\omega) \in \mathbb{R}^n \qquad (\tau = \omega t). \tag{2.3}$$

Then $q(\cdot)$ is stationary [2] for $\mathcal{T}_h$ if and only if $\bar{q}(\cdot)$ solves the Lagrange equations for $L = K - V$ with total energy $E = K + V = h$. The value of ω, involved in (2.3), is determined only by the knowledge of $q(\cdot)$ and h.

A direct computation will prove our assertion:

$$\begin{aligned}
\delta J_h(q)\delta q &= \frac{d}{d\lambda}\left\{ \int_0^1 K\big(\dot{q}(\tau) + \lambda\delta\dot{q}(\tau)\big)\, d\tau \cdot \int_0^1 \Big(h - V(q(\tau) + \lambda\delta q(\tau))\Big)\, d\tau \right\}\Bigg|_{\lambda=0} \\
&= \int_0^1 \nabla K(\dot{q}(\tau))\delta\dot{q}(\tau)\, d\tau \cdot \int_0^1 (h - V(q(\tau)))\, d\tau - \\
&- \int_0^1 K(\dot{q}(\tau))\, d\tau \cdot \int_0^1 \nabla V(q(\tau))\delta q(\tau)\, d\tau
\end{aligned} \tag{2.4}$$

so the curve is critical if and only if:

$$\omega^2 \int_0^1 \nabla K(\dot{q}(\tau))\delta\dot{q}(\tau)\,d\tau - \int_0^1 \nabla V(q(\tau))\delta q(\tau)\,d\tau = 0 \tag{2.5}$$

where,

$$\omega^2 := \frac{\int_0^1 (h - V(q(\tau)))\,d\tau}{\int_0^1 K(\dot{q}(\tau))\,d\tau} \tag{2.6}$$

This means that $q(\cdot)$ must be a solution of:

$$\omega^2 \frac{d^2q}{d\tau^2}(\tau) + \nabla V(q(\tau)) = 0 \tag{2.7}$$

We remark that the above calculation actually shows only that $q(\cdot)$ is a weak solution of this system of differential equations. But under our regularity assumption on the potential we can invoke standard theorems to claim that it is also a classical $\mathcal{C}^2$ solution. Moreover $J_h(q(\cdot)) > 0$, then the above ω^2 is a positive real number, so by performing the linear time reparametrization

$$[0, \omega^{-1}] \ni t \mapsto \tau(t) = \omega t \in [0, 1]$$

we see that $\bar{q}(t) = q(\omega t)$ solves the *mechanical* Lagrange equations:

$$\frac{d^2\bar{q}}{dt^2}(t) = -\nabla V(\bar{q}(t)) \tag{2.8}$$

Finally, recalling the conservation of energy for $\bar{q}$, and denoting by E the related total energy value,

$$E = \left(K(\frac{d\bar{q}}{dt}(t)) + V(\bar{q}(t)) \right)\Big|_{t=\tau\omega^{-1}} = \omega^2 K(\frac{dq}{d\tau}(\tau)) + V(q(\tau)),$$

By integration on τ:

$$\int_0^1 \big(E - V\big)d\tau = \omega^2 \int_0^1 K d\tau,$$

And so the total energy E of the curve we have found is exactly the value h imposed from the beginning.

3. Finite Dimensional Reduction. We present a modification of the classical Amann-Conley-Zehnder reduction technique [5]. Here reduction means that we are able to transform a problem defined over a (infinite dimensional) functional space into an algebraic one with a finite number of unknowns. We will show how to handle the time reparametrisation of the Tonelli functional in this framework. In the next paragraph we apply this theoretical tool to the numerical calculation of stationary points. The description of the procedure has to be very technical. However, the main idea is quite simple: knowing only the first N Fourier components of the solution (i.e. solving system 3.12), with this reduction technique, we can reconstruct the entire series. The engine of this machinery is a contractive map defined on the queues (3.7) that gives the remaining (infinite) components of the solution as its unique fixed point.

The choice of the (truncated) Fourier series for the discretization of the problem may not be the optimal one, from the computational point of view. A trajectory described in terms of cartesian coordinates at fixed time steps, and/or in terms of splines joining them allows for more efficient numerical techniques for functional stationarization. We will remark this also in the following section. However, the Fourier description represents for the moment the best compromise between theoretical needs and computational costs. Indeed, the finite reduction technique -although it predicts exactly positions and velocities- involves integral properties of the function describing the trajectory (originally it involved the eigenfunctions of the differential operator employed and also recent studies [6] highlight the advantages of a Fourier decomposition). The results of the simulations described later in the paper are satisfactory, in our opinion. Notwithstanding this, we are investigating deeper the problem and this will be a preferred direction in our future work. Moreover, we point out that alternative expansions like spline interpolation could be investigated and their efficiency compared with the Fourier expansion.

3.1. Hypothesis and preliminary considerations. The main hypothesis under which this developing theory does work, is that the potential should have an uniformly bounded Hessian. From the physical point of view, this means that we can concern with any non-linear force with the only prescription that if it diverges, it goes to infinity at most linearly. However, its potential is not necessary convex there.

The value of ω appearing in (2.7) is at the starting point an unknown. Thus in the study of the lagrangian $\tilde{L} = K - \frac{V}{\omega^2}$, we will treat this value as a parameter of the problem satisfying equation (2.6) (see also (3.4) below). As before we consider the boundary data $q(0) = q_0$ and $q(1) = q_1$, but for this procedure we need functions with more regularity so we will work in

$$\Gamma' = \{q(\cdot) \in H^2((0,1), \mathbb{R}^{3\mathcal{N}}) : q(0) = q_0, \quad q(1) = q_1\}.$$

A function $q \in \Gamma'$ is in particular a function in L^2 for which a Fourier decomposition is available. Before entering in the mathematical details, it is important to notice that the regularity assumptions in the definition of Γ' and the boundary data are sufficient to assure the existence of the second derivative of q and to allow us its calculation by a term by term derivation in the Fourier series. A simple choice for the representation is:

$$q(t) = q_0 + (q_1 - q_0)\, t + \sum_{n \in \mathbb{N}} a_n \sin(\pi n t) \tag{3.1}$$

This is not a traditional Fourier series, but it is a standard choice in path integral formulations: it appeared already in the physics book by Feynman [7] and more recently it was used by Doll in different works, see for example [8, 11]. The convergence of this series to the original function in the H^2 norm is straightforward in Fourier analysis. The idea is to extend any function to an odd function in $(-1, 1)$ and then to use the standard Fourier series on it. We recall the main features of this decomposition.

(i) The function $q(t) - q_0 - (q_1 - q_0)\, t$ is, under our assumptions, in H_0^2; so we can surely write $q(0) = q_0$ and $q(1) = q_1$. This is due to the standard Sobolev embedding theorem.

(ii) $-\sum \pi^2 n^2 a_n \sin(\pi n t)$ converges to $\ddot{q}$ in L^2, by Poincaré inequality. Indeed $q - q_{\bar{n}} := q - \Big(q_0 + (q_1 - q_0)\, t + \sum_{n \le \bar{n}} a_n \sin(\pi n t)\Big)$ is a function in H_0^2 which tends to zero in L^2 as $\bar{n}$ goes to infinity with its first two derivatives.

(iii) This last convergence result does not imply that $\ddot{q}$ is zero at the boundary, in fact here we cannot invoke any embedding theorem and so we do not have any information on the local behavior of the second derivative. The Fourier series converges only at almost every point (with respect to the Lebesgue measure).

3.2. Mathematical structure. With the proposed parametrization, if we put $\phi = \sum_{n\in\mathbb{N}} a_n \sin(\pi n t)$ in (3.1) we can rewrite the equation for the modified Lagrangian system as:

$$\ddot{\phi} = -\frac{\nabla V(q)}{\omega^2} \tag{3.2}$$

Now we can start the reduction procedure; we have to fix a number N and to split the space where $\ddot{\phi}$ lies in the following way: for any $\psi \in L^2((0,1),\mathbb{R}^{3\mathcal{N}})$ we put

$$\mathbb{P}_N\psi(s) := \sum_{n\le N} \psi_k \sin(\pi n s), \qquad \mathbb{Q}_N\psi(s) := \psi(s) - \mathbb{P}_N\psi(s), \tag{3.3}$$

so we can write $L^2 = \mathbb{P}_N L^2 \oplus \mathbb{Q}_N L^2$ and we will call u the finite part, v the infinite one. This is the announced separation between the finite part of the series (up to order N) and the infinite dimensional space of the queues. When no confusion can possibly arise, we will often call with the same name the function and the coefficients of the Fourier series. For technical and practical reasons, that will be immediately clarified, we need also to keep the u component together with the real parameter ω: we will call $\bar{u}$ the pair $(\omega, \mathbb{P}_N\phi) \in \mathbb{R}\times\mathbb{P}_N L^2$. So, summing up, our set of unknowns is

$$(\bar{u}, v) = (\omega, u, v) \in \mathbb{R}\times\mathbb{P}_N L^2 \times \mathbb{Q}_N L^2 \tag{3.4}$$

For any fixed value of $\bar{u}$, we introduce the functional

$$G : \mathbb{Q}_N L^2 \longrightarrow \mathbb{Q}_N L^2 \tag{3.5}$$

$$v \longmapsto G(v) \tag{3.6}$$

where the n-th component of $G(v)$ in the sine basis is defined by

$$[G(v)]_n := \frac{1}{(\pi n)^2}\left[\frac{\nabla V\left(q_0 + (q_1 - q_0)\,t + u + v\right)}{\omega^2}\right]_n \qquad \text{for } n > N \tag{3.7}$$

We can show that if N is large enough the map G is a contraction between Banach spaces and thus it admits one, and only one, fixed point. We prove this with a direct computation, but first we recall how it is possible to calculate the norm of an L^2 function using its Fourier coefficients. For any function $\psi \in L^2((0,1),\mathbb{R}^{3\mathcal{N}})$ we can write:

$$\|\psi\|_{L^2} = \left(\int_0^1 |\psi(t)|^2_{\mathbb{R}^{3\mathcal{N}}}\,dt\right)^{\frac{1}{2}} = \left(\int_0^1 \sum_{i=1}^{3\mathcal{N}} \psi_i^2(t)\,dt\right)^{\frac{1}{2}} \tag{3.8}$$

$$= \left(\sum_{i=1}^{3\mathcal{N}} \int_0^1 \psi_i^2(t)\,dt\right)^{\frac{1}{2}} = \left(\sum_{i=1}^{3\mathcal{N}}\sum_{n=1}^{+\infty}\int_0^1 a_{in}^2 \sin^2(\pi n t), dt\right)^{\frac{1}{2}} \tag{3.9}$$

$$= \frac{1}{\sqrt{2}}\left(\sum_{i=1}^{3\mathcal{N}}\sum_{n=1}^{+\infty} a_{in}^2\right)^{\frac{1}{2}} \tag{3.10}$$

where we have introduced the Fourier representation $\psi_i(t) = \sum_n a_{in} \sin(\pi n t)$. Applying this result to our function G, we can prove the desired inequality. In the following calculation we write $\phi_0 = q_0 + (q_1 - q_0)t$, $C = \sup_{x \in \mathbb{R}^{3\mathcal{N}}} |\nabla^2 V(x)| < +\infty$ and we keep together the three spatial coordinates of G avoiding heavy notations. Thus we have:

$$\begin{aligned}
\|G(v_2) - G(v_1)\|_{L^2} &= \frac{1}{\sqrt{2}} \left(\sum_{n>N} |\, [G(v_2)]_n - [G(v_1)]_n \,|^2 \right)^{1/2} \\
&= \frac{1}{\sqrt{2}} \left(\sum_{n>N} \frac{1}{(\pi n)^2} \left| \left[\frac{\nabla V(\phi_0 + u + v_2)}{\omega^2} \right]_n - \left[\frac{\nabla V(\phi_0 + u + v_1)}{\omega^2} \right]_n \right|^2 \right)^{1/2} \\
&\leq \frac{1}{\pi^2 (N+1)^2 \omega^2 \sqrt{2}} \left(\sum_{n>N} |[\nabla V(\phi_0 + u + v_2) - \nabla V(\phi_0 + u + v_1)]_n|^2 \right)^{1/2} \\
&\leq \frac{1}{\pi^2 (N+1)^2 \omega^2} \|\nabla V(\phi_0 + u + v_2) - \nabla V(\phi_0 + u + v_1)\|_{L^2} \\
&\leq \frac{C}{\pi^2 (N+1)^2 \omega^2} \|v_2 - v_1\|_{L^2}
\end{aligned} \tag{3.11}$$

If N is large enough, we will have $\alpha := \frac{C}{\pi^2 (N+1)^2 \omega^2} < 1$ and G is a contraction. By standard arguments we can deduce now the existence of a unique fixed point: $f(\bar{u}) = G(f(\bar{u})) \in \mathbb{Q}_N L^2$. We remark that $\bar{u} \mapsto f(\bar{u})$ is of class C^1, as we can prove with the implicit function theorem.

With this function the variational problem can be translated into an algebraic one. In fact, now we have only to solve the following finite dimensional system, where we mean $u = \sum u_n = \sum a_n \sin(\pi n t)$ and $1 \leq n \leq N$:

$$\begin{cases}
a_n &= \dfrac{1}{(\pi n)^2} \left[\dfrac{\nabla V(\phi_0 + u + f(\bar{u}))}{\omega^2} \right]_n \\
\omega^2 &= \dfrac{\int_0^1 (h - V(\phi_0 + u + f(\bar{u})))\, d\tau}{\int_0^1 K\left(\frac{d}{dt}(\phi_0 + u + f(\bar{u}))(\tau) \right) d\tau}
\end{cases} \tag{3.12}$$

If we are able to find a solution, we will gain the corresponding mechanical curve: first, we pass the factor $(\pi n)^2$ to the left hand side of each component of $(3.12)_1$ and of (3.7); then, we observe that $-(\pi n)^2 u_n$ for $1 \leq n \leq N$, and $-(\pi n)^2 f(\bar{u})_n$ for $n > N$, make up precisely the Fourier components of $\ddot{\phi}$. Finally we recover $\ddot{\phi} = -\frac{\nabla V(q)}{\omega^2}$ with the correct value of the parameter ω found in (3.12).

3.3. The reduction for the harmonic oscillator. The harmonic oscillator shows very well the role of the parameters of the procedure and the meaning of the bounds that we have to impose on them. The interesting point is the condition for the contraction: the theory says that we can always take an N large enough, but if ω is too small, the value reached by the number of Fourier coefficient is out of any computational purpose. Moreover, as we will discuss later, the analysis of this example enters in the fine details of the structure of the problem.

Let us consider the classical harmonic oscillator of equation $\ddot{q} + kq = 0$. We compute the contraction coefficient for this case: the period of an oscillation is $T = \frac{2\pi}{\sqrt{k}}$, the supremum of the Hessian of the potential is $C = k$, hence

$$C = \frac{(2\pi)^2}{T^2} \tag{3.13}$$

Denoting by $T_\omega = \frac{1}{\omega}$ the total time related to ω in the Tonelli functional (2.3), we have

$$\alpha = \frac{4}{T^2(N+1)^2\omega^2} = \frac{4T_\omega^2}{T^2(N+1)^2} < 1 \tag{3.14}$$

so the contraction works if

$$N + 1 > 2\frac{T_\omega}{T} \tag{3.15}$$

We remark that in this case this estimate is sharp. In fact if we consider a trajectory whose time length is less than half of a period T, the estimate tells us that $N = 0$ is admissible and so we can compute all the Fourier coefficients with the contraction. On the other hand, if the time length is over $T/2$, we need at least $N = 1$. This coincides with the theory of conjugate points: exactly at half of a period the first conjugate point appears. We know that after it the trajectory is no more a minimum for the action functional and we cannot expect that the contraction will converge with $N = 0$. From this we learn that in more complex cases we must take care about the product $\omega(N+1)$: for any chosen value of N, there is a largest value of the trajectory total time ω^{-1} that we cannot overcome without losing the contractivity.

4. Performance of Tonelli principle and comparison with Maupertuis principle. The most popular variational principle that allows to obtain trajectories at fixed energy is based on the following functional:

$$\mathcal{M}_E(q(\cdot)) = \int_0^1 \sqrt{2(E - V(q(\tau)))\, m\, |\dot{q}(\tau)|^2}\, d\tau. \tag{4.1}$$

The relation between the geometric and the real time is generically not linear, whereas in Tonelli principle it is an uniform reparametrization. *The theory tells us that -although it is not defined over all the configuration space- $\mathcal{M}_E$ offers directly a geometric formulation of the problem in terms of a Riemannian metric and its geodesics. Unfortunately this metric becomes singular whenever $V(q(\tau))$ approaches (from below) E. Moreover in these situations the precision of the parametrization decreases and this can be highlighted in any standard numerical implementation of this principle.* We show this with a simple example: a one-dimensional double well.

Both principles (Tonelli and Maupertuis) are translated into algorithms with similar techniques as the ones described in [21]: the path is discretized and the functional optimization is transformed into an optimization of a discretized action, function of the internal degrees of freedom of the path (the extremes and the total energy are kept fixed). In our case we set $V(q) = 0.25 \times q^4 - 0.5 \times q^2$, with two minima at $q = \pm 1$ and a central transition state with zero potential energy. If necessary, we also use a Monte Carlo based simulated annealing with the norm of the gradient (see later in this paper, eq. (6.1) for Tonelli's case; the implementation for Maupertuis principle

is similar) as objective function. This procedure showed more stability with respect to conjugate residual in the case of Maupertuis principle.

We set the fixed extremes q_0 and q_1 in the two basins of the potential, and we consider as trial trajectory a linear interpolation between q_0 and q_1. As a first test, we notice that we can find a solution with any desired positive energy using Tonelli principle, both starting from the linear interpolation and from a random perturbation of a known solution (e.g., a solution that "bounces" on the walls of the well before the transition).

In general, the same success is obtained also with Maupertuis principle, with some important exceptions. We will indeed focus on the particular cases where the total energy is very close to the barrier. All our simulations were performed with 200 intermediate slices.

In fig. 4.1 we show the solution of Tonelli principle (top panel, above) and the one of Maupertuis principle (top panel, below) for a total energy of $E = 0.1$, using a starting path already close to the solution. The solutions on this panel correspond to a total time of $\tau = 6.67$. We verified separately (using Hamilton principle) that this total time is correct for such energy.

The only difference between the two subpanels can be seen in the region where kinetic energy is small. Whereas Tonelli principle describes the whole potential profile around the maximum in an accurate manner, the time dilation inherent to the geometric trajectory leads to a poor sampling of the region around the barrier in the Maupertuis case.

If the total energy is decreased, and we start already close to the solution, both principles behave more or less in the same correct matter. When $E \simeq 10^{-4}$, the precision of Maupertuis principle is better than the one on Tonelli's: in this particular case, the resulting trajectories from Tonelli principle correspond to a total energy smaller than the prescribed value. We found empirically that the error on the total energy for the Tonelli functional is of the order of $\Delta E \simeq 8 \times 10^{-5}$. We are presently investigating the numeric origin of this systematic error.

A more serious problem is represented by the fact that Maupertuis functional has a delicate behavior (due to the presence of the square root of the difference $E - V$) in the proximity of the barrier. We show here an example starting from a linear trial path randomized with an amplitude $\Delta x = 0.2$. The optimization with Tonelli principle leads to a correct trajectory with the prescribed energy of $E = 0.01$, whereas Maupertuis principle suffers from the fact that the time intervals are derived point by point in the path from the ratio between geometric kinetic energy and square root of energy difference $\sqrt{E - V(q)}$. Since the geometric kinetic energy is calculated by finite difference on a noisy trajectory, the fluctuations in the path are going out of control: the result of the failed optimization of the path is shown in fig. 4.1, bottom panel. This failure calls for more suitable algorithms based on a multi-scale calculation of the kinetic energy; this is not needed in the case of Tonelli principle. An additional problem in the Maupertuis functional is represented by the timestep dilatations in the vicinity of the barrier. Such time dilatations are inversely proportional to $\sqrt{E - V(q)}$.

4.1. Mueller potential. In this section we test the Tonelli functional with the widely known two-dimensional Mueller potential [9]. It is a popular test case for reaction path methods; its analytic form can be found for example in eq. 4 of the Bai and Elber paper [16], and it has three minima and two main transition states.

In their paper, Bai and Elber noticed that for each total energy or total time, several different paths are possible, and that not all the energies are available for paths

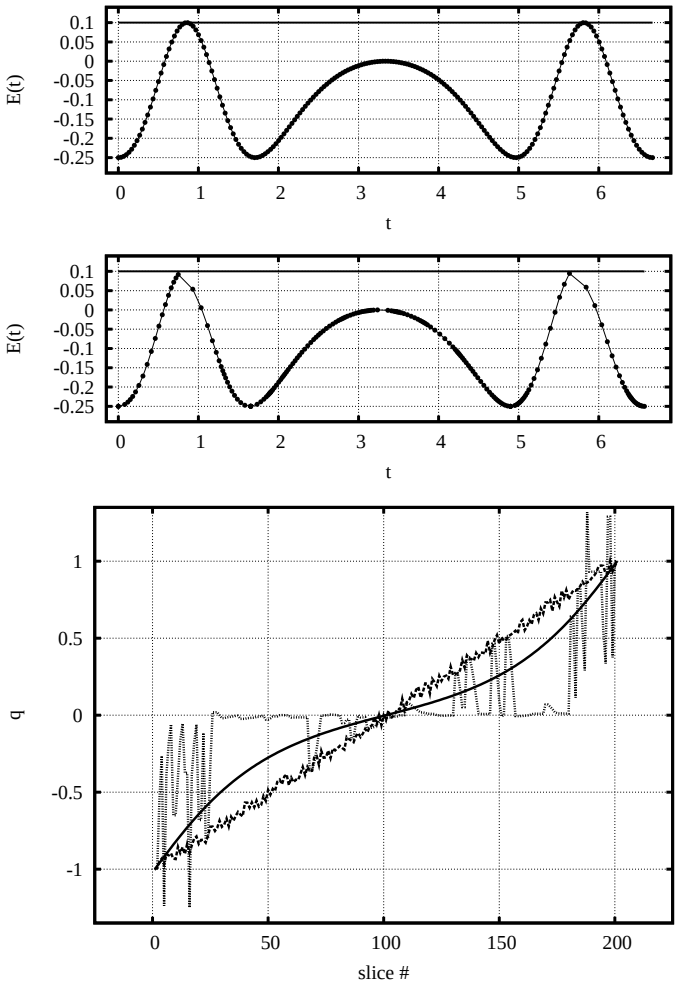

FIGURE 4.1. *Comparison between Tonelli and Maupertuis functional in finding trajectories at total energies close to the barrier. top panel: energies obtained from Tonelli functional, starting from good or randomized guesses, at* $E = 0.1$ *(above) and Maupertuis functional, starting from good or randomized guesses; bottom panel: failed Maupertuis optimization (dotted line) and Tonelli optimization (continuous line), starting from a randomized guess (dashed line), at* $E = 0.01$*. In this case, the coordinate as a function of path slice is shown. The total time is the correct value of* $\tau = 5.59$ *for the optimized Tonelli path and a exceedingly large value of* $\tau = 74$ *for the Maupertuis path which did not reach convergence in this case.*

with a given total time. Using Tonelli principle we will show that it is possible to obtain different paths with the same energy, joining the same endpoints; moreover, we underline a difficulty of energy-based variational principles: it is not granted that local optimizers can find solutions with a requested energy. Instead, a given path basin can contain trajectories with other energies, that can be still found using Tonelli principle with another prescribed total energy.

To illustrate the first point, we first generated a relatively high energy trajectory ($E = -11.5$) using a Verlet algorithm with a timestep $\Delta t = 0.003$. Using this trajectory as starting point, we run a simulated annealing procedure using as target

function the sum of squared residual errors on Tonelli's equations of motion. We use 150 intermediate slices, for a total of 300 degrees of freedom.

Depending on the simulated annealing protocol, the algorithm ends close to the original path or in another basin of attraction. A refinement using the conjugate residual method [22] leads in both cases to a solution of Tonelli principle. But as it can be seen from figure 4.2, the two solutions are different, although with the same energy.

The same exercise repeated with Maupertuis principle succeeds in finding again the original Verlet path, but not in reaching another basin of attraction and a different trajectory with the same energy.

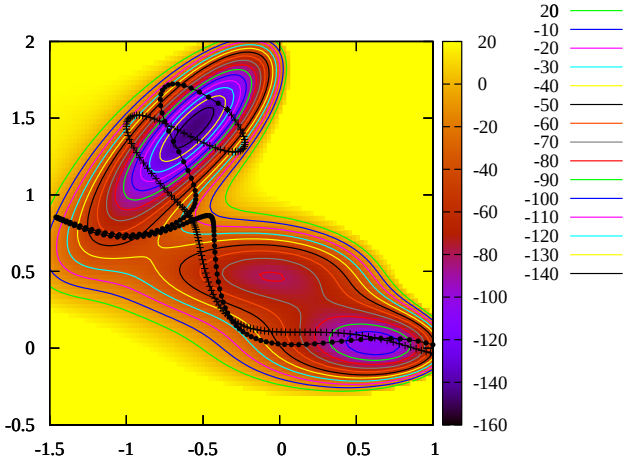

FIGURE 4.2. *Two trajectories in the Mueller potentials, one obtained with Verlet integration (crosses), the other one (points) obtained from the former with Tonelli principle and simulated annealing. Both trajectories have an energy* $E = -11.5$*, and the same extremes.*

The second attempt was to obtain a completely new path starting only from the knowledge of the extremes. First of all, we generated a trial path by linear interpolation between the two main minima. Starting from the straight path, we run a simulated annealing procedure using as target function the sum of squared residual errors on Tonelli equations of motion.

We set at total energy a value $E = -40$, just above the position of the main transition state. We divide our path in 50 slices, for a total of 100 degrees of freedom. After the simulated annealing procedure, we use a conjugate residual method in order to refine the solution. We observe that with the prescribed value of the energy, we could not find a solution close to the outcome of the simulated annealing. Conversely, if the conjugate residual is applied to the same starting point, but using Tonelli principle with a energy larger than a certain threshold ($E > -28$ in this case), the local optimization algorithm is able to find a solution of Tonelli principle, shown in the figure for the limiting case $E = -28$.

As a check, we apply Hamilton's principle to the optimized trajectory. We impose a fixed total time, and we obtain the trajectory outlined in figure 4.3, which has a

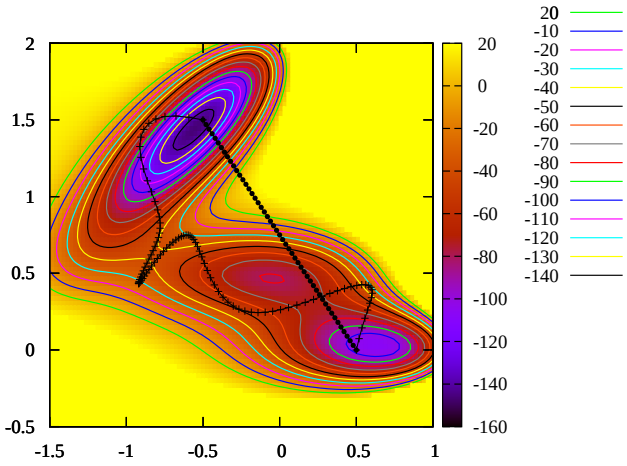

FIGURE 4.3. *Trajectory in the Mueller potential (crosses) obtained from the linear interpolation (points), using Tonelli principle and the simulated annealing algorithm followed by a conjugate residual refinement. The trajectory has a total energy of* $E = -28$.

conserved energy of $E = -28$.

The optimization using Maupertuis principle could not lead in this case to a solution of the problem, due to the already sketched difficulties related with the term $(E - V)$ in the denominator of the gradient of the functional.

It could well be that Maupertuis principle can be used with more clever algorithms, but we want to stress here that the tool of Tonelli's optimization allows to explore the possibility of transition paths at different energies in a controlled way. In our opinion, the main obstacle to the future application of Tonelli principle in general is how to know at the *beginning* of the optimization process that a path with a prescribed energy is not available in a certain region of trajectory space.

5. An algorithm for the contraction. We realize that the instabilities and the problems related to the functional $\mathcal{M}_E$ could be overcome by the development of some suitable clever algorithms. We tried some of them (for example the use of penalty functions for avoiding the explorations of regions where $V(q) > E$) but failed to find sufficiently general strategies. In this paper, with the introduction of $\mathcal{T}_h$, we propose instead a different approach that relies on standard optimization algorithms and couples Tonelli principle with the finite reduction.

We can schematize our algorithm as follows:

(i) set q_0 and q_1, the initial and final points of the trajectory;

(ii) find an initial path π_0 connecting q_0 and q_1. This can be a linear interpolation, or an approximation to a minimum energy path with a few intermediate images; the latter approach gives a reasonable estimate of the maximum value of the potential energy V_{max};

(iii) discretize π_0 into M slices;

(iv) set the total energy E at a value larger than V_{max};

(v) extract the finite reduction threshold N from the contraction condition

(3.11) this condition requires an estimate of the supremum of the Hessian in the potential;

(vi) *start iteration:* expand the path π_0 in Fourier series, and keep the first N harmonics. This generates the finite dimensional system (3.12), that can be solved using iterative methods like the conjugate residual [22]. In the first step, set the harmonics $N+1$ to M to zero, corresponding to setting $f(u) = 0$ in eq. (3.12). Only a few steps of conjugate residual are performed, this generates a new path $u_1 = \sum_1^N a_n \sin(\pi n t)$;

(vii) u_1 is inserted into (3.7), which is a contraction if N was carefully chosen. That leads to a set v_1, which can be referred to as the Fourier components $N+1$ to M of the trajectory;

(viii) the new path π_1 is found as $\pi_1 = u_1 + v_1$;

(ix) in (3.12), set $u = u_1$, $f(u) = v_1$; the second equation in the system also provides the total time of the path;

(x) check whether the threshold N still leads to a contraction using the estimate (3.11);

(xi) iterate the procedure until convergence.

5.1. Error estimates. In the next section we will show a test case for this procedure, but first we want to test the quality of a generic trajectory computed with this algorithm. The first step is to compute the error made by considering our truncated contraction, say $f_{N,M}(\bar{u}) = G_{N,M}(f_{N,M}(\bar{u}))$, with respect to the real one. We denote α the contractive constant in (3.11):

$$\begin{aligned}\|f_{N,M}(\bar{u}) - f(\bar{u})\| &= \|G_{N,M}(f_{N,M}(\bar{u})) - G(f(\bar{u}))\| \\ &\leq \|G_{N,M}(f_{N,M}(\bar{u})) - G_{N,M}(f(\bar{u}))\| + \|G_{N,M}(f(\bar{u})) - G(f(\bar{u}))\| \\ &\leq \alpha\|f_{N,M}(\bar{u}) - f(\bar{u})\| + \|G_{N,M}(f(\bar{u})) - G(f(\bar{u}))\|\end{aligned} \tag{5.1}$$

Hence:

$$\begin{aligned}\|f_{N,M}(\bar{u}) - f(\bar{u})\| &\leq \frac{1}{1-\alpha}\|G_{N,M}(f(\bar{u})) - G(f(\bar{u}))\| \\ &= \frac{1}{1-\alpha}\|\mathbb{Q}_M G(f(\bar{u}))\| = \frac{1}{1-\alpha}\|\mathbb{Q}_M f(\bar{u})\|\end{aligned} \tag{5.2}$$

With this information, calling q the real trajectory, $\tilde{q}$ a curve with M Fourier components (that is stationary for the M-discretized Tonelli functional) and $\bar{q}$ a curve obtained with our procedure we get:

$$\|q - \bar{q}\| = \|q - \tilde{q} + \tilde{q} - \bar{q}\| \leq \frac{2-\alpha}{1-\alpha}\|q - \tilde{q}\| \tag{5.3}$$

This means that we can obtain an error with the same order of magnitude of the traditional stationarization, but following a more efficient and quicker path. Numerical evidence of this are presented in the next section.

6. Test cases. The following tests implement the finite reduction strategy outlined in the mathematical sections of the present paper.

6.1. 4 Atom Lennard-Jones cluster. Here we will present a simple system and we will show in details the implementation of the algorithm. The system is a concrete one (a cluster of four atoms interacting through a Lennard-Jones potential),

but it is not interesting for its features: for the moment we do not want to overlap difficulties arising from the algorithm with the intrinsic problems of a more complicated (and interesting) system.
The trajectory we want to reproduce is a short oscillation of four atoms (that could model a small argon cluster). The path of a classical Verlet simulation (in the initial value representation) is drawn in figure 6.1 (for one coordinate), and the total time is $\tau = 2$ in Lennard-Jones units.

In order to test the contraction strategy, we set the two extremes of this trajectory, and we perturb the trajectory. That is, we change the trajectory randomly keeping the extremes fixed. Not only, but we also apply a randomization to the u and v components. The trajectory after randomization is shown (for the same coordinate as before) in figure 6.1. Larger randomizations in such a small total time could be hard to recover. A datum not present in the picture is that, after the randomization, the total time has increased to $\tau = 12$ in Lennard-Jones units.

Now we set an N to divide the u components and the v components. In this case as an illustration we use $N = 30$. First of all, we apply an algorithm to the u components, for lowering a bit the potential energy. This is done by inverting the sign of the potential energy. Then we set the total energy to the -4.49 value of the original trajectory. We apply the equations of Tonelli for the u for 10 iterations. We obtain a set of u that, together with the set of v coming from the randomization, give the trajectory in figure 6.1. Here the total time is 4 times the correct one.

Then we apply the contraction to the v. This contraction is applied in presence of a u that is not yet the correct solution. Nevertheless, we must obtain a fixed point. The interesting thing is that already after this first iteration, the error on the highest harmonics has decreased considerably.

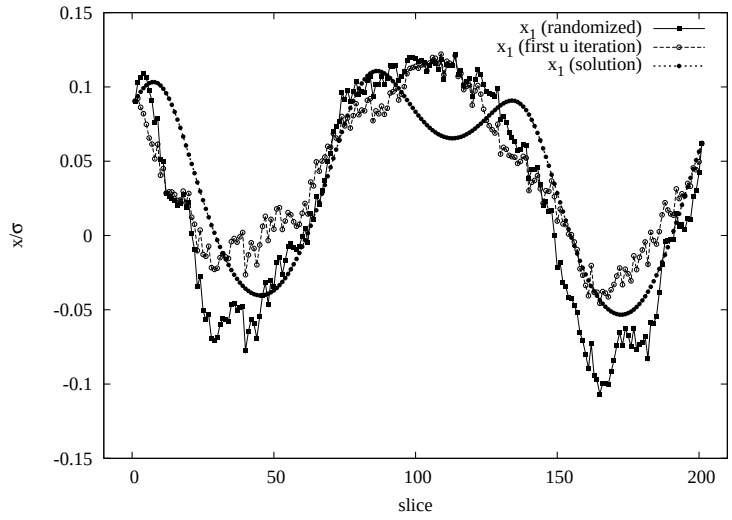

FIGURE 6.1. *The coordinate x of atom 1 (final solution, randomized, after the first u-iteration)*

We can now repeat the same procedure of optimization for u and the contraction, iteratively, and we succeed in optimizing the trajectory. After 3 cycles of (30 cycles of u optimization + contraction) we reached the energies (potential and total), and the error on the highest harmonics plotted on figure 6.3 and 6.4.

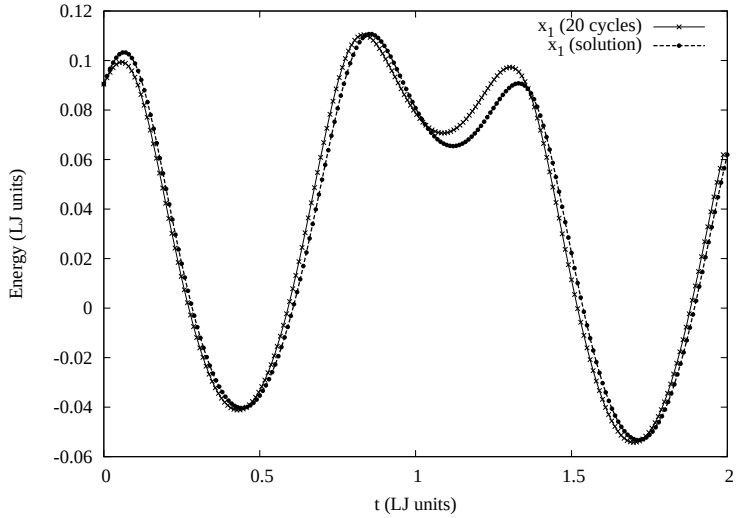

FIGURE 6.2. *The coordinate x of atom 1 (final solution and after 20 cycles of u-optimization/contraction)*

At this point the situation has improved, and even more after twenty of such cycles. The whole series of cycles takes less than 3 minutes on a normal laptop: it is a small system indeed. This final result is shown in figures 6.2 (for the x coordinate of atom 1) and 6.4 (for total and potential energies).

We find that the trajectory is very close to the correct one. The error on the trajectory (the norm of the errors on Newton equations along the path) has decreased by several orders of magnitude throughout the procedure. The total energy, computed from derivation of the Fourier series, averages to the value requested by Tonelli principle, by construction. The oscillations are due to the kinetic energy, since very small displacements in the coordinates can produce large oscillations in the kinetic energy.

6.2. 38-atom Lennard-Jones Cluster. A far more demanding case is the isomerization of a 38 atom Lennard-Jones (LJ) cluster. This system is a traditional benchmark both for algorithms aiming at minima localization in a potential energy surface (PES) and for methods for extracting statistical quantities using path sampling. The PES of this system has moreover a double funnel structure, which can be seen as a "toy model" for the protein folding scenario. Recently, Bai and Elber have developed a novel strategy for sampling very short dynamical paths [16]. In that paper, they discuss the importance of short time trajectories in the frame of path sampling. We will not consider that issue here. However, as discussed in the introduction, we point out that an algorithm that allows to obtain trajectories at a given energy could also be of importance in a sampling procedure including the total energy as external parameter, as in the Wang-Landau method [17], where the sampling is enhanced in energy regions that are infrequently visited in a traditional Monte-Carlo method.

Bai and Elber considered different test cases for their algorithms. For systems with few degrees of freedom (like the Mueller potential) they show in their paper the efficiency of a particular refining procedure based upon the knowledge of the Hessian

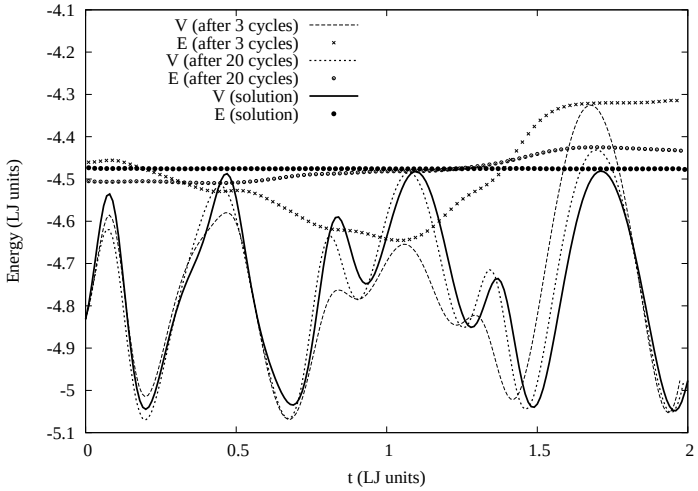

FIGURE 6.3. *Potential and total energy for the total trajectory after 3 and 20 cycles of finite reduction, compared with the exact solution.*

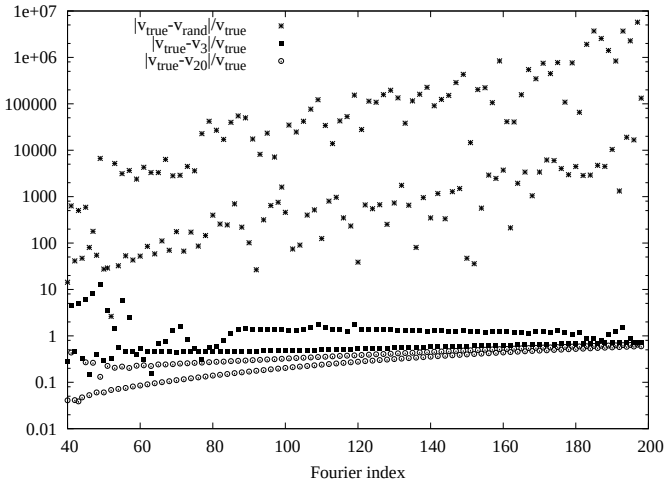

FIGURE 6.4. *Error on the higher harmonics for the x coordinate of atom 1, after randomization, 3 cycles, and 20 cycles of finite reduction.*

matrix (Kaczmark iterations). This procedure, however, has a sizeable computational cost, and as soon as a larger system is concerned, the authors do not apply it there. Bai and Elber were able to find reactive trajectories (although with a limited number of intermediate points) for a fascinating and realistic system: they applied their method to the fast transitions between a face-centered cubic and an icosahedral structure in a solid cluster made by Argon atoms. This system can be modeled by a pairwise Lennard-Jones potential, with parameters $\sigma = \varepsilon = 1$. The authors use a standard algorithm, a simulated annealing procedure and they are able to obtain trajectories with different total times (and 32 slices), starting from a linear interpolation between the two absolute minima of the potential energy surface (fcc and icosahedral).

We took inspiration from this test case, with some modifications in the optimiza-

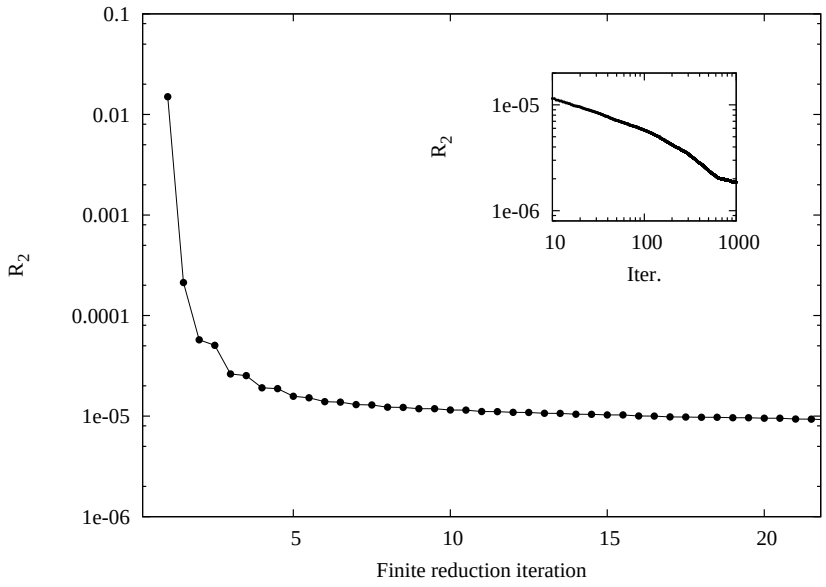

FIGURE 6.5. *The convergence of the squared residual R_2 for the path at $E = -110$ during the finite reduction iteration. Starting from the final value obtained from simulated annealing for the 32 slice path, the residual rapidly decreases and slowly reached the value $R_2 = 0.2 \cdot 10^{-5}$ (see inset).*

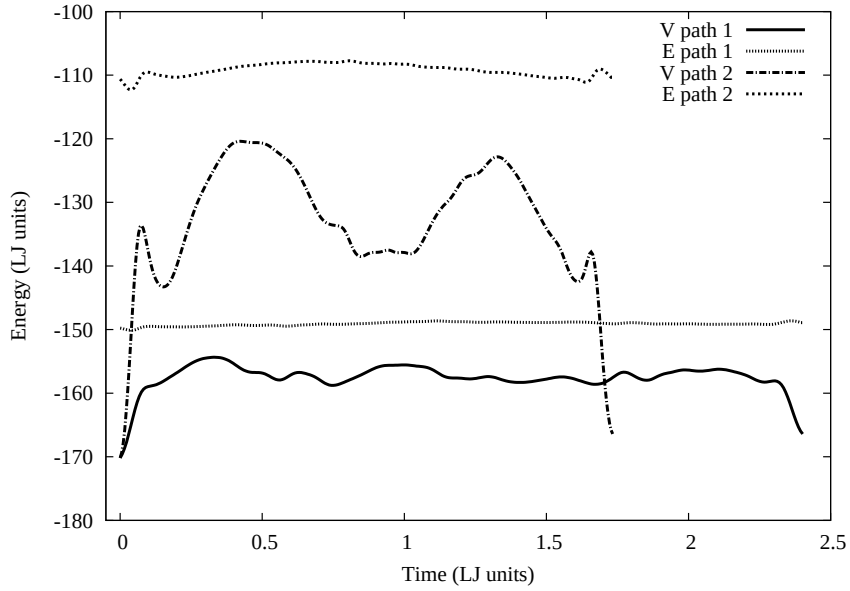

FIGURE 6.6. *Potential and total energies for the paths at fixed total energies $E_f = -110$ and $E_f = -150$, after finite reduction with $M = 320$ total number of harmonics.*

tion protocol. First of all, our starting point was an approximation to the minimum energy path (MEP), obtained by applying Tonelli principle with a "total energy" which is lower than all the potential energies of the system (it is a computational artifact to obtain a trajectory with inverted sign potential, see the discussion in [12]). The energy of the two minima is -174 (LJ units), whereas the transition state is at

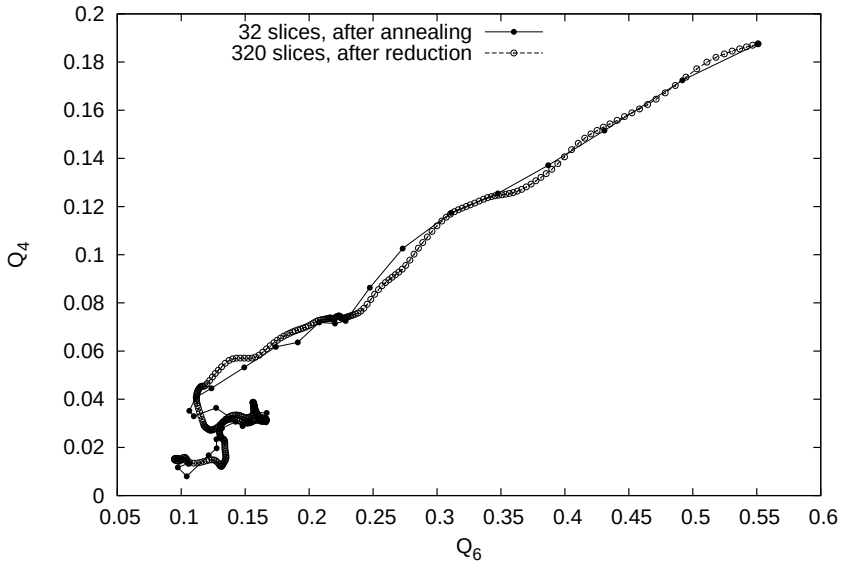

FIGURE 6.7. *Comparison between the orientational order parameters [23] for the coarse trajectory obtained after annealing (32 slices at $E_f = -150$) and the subsequent finite reduction with iterations at the same energy.*

about -158. By comparison, the lowest energy path between the two basins, obtained with eigenvector following by Doye and coworkers [23], has an height of -169.7. Here, we are only interested in a good starting point for our procedure. Starting from this low energy path, we adopt a simulated annealing procedure as in [16] using as target function the sum on the squared residual R_2 of the equations of motion:

$$R_2 = \sum_{l=1}^{M-1} \left(q_{l+1} + q_{l-1} - 2q_l + m^{-1}\Delta^2 \frac{\partial V}{\partial q_l} \right)^2 \tag{6.1}$$

(with obvious extension to the multidimensional case) where M is the number of time slices and $\Delta = T_\omega / M$.

In order to find two different paths we run two different simulated annealing protocols, setting the total energy to $E_f = -150$ and to $E_f = -110$, respectively. At each Metropolis step we recalculate the total time T_ω using eq. (2.6). During the minimization of the residuals, the average total energy remains fixed at E_f , as it can be easily derived from the form of Tonelli functional. After simulated annealing, our 32 slices trajectories have a residual of 0.01 and 0.004, respectively. The total energy is well conserved in both cases, and the total time is $\tau = 2.4$ and $\tau = 1.5$ in the two cases.

At this point we plan to use the finite reduction procedure in order to increase the number of slices. We start from a linear interpolation of the 32 slices, and we get a path with 320 slices. With the goal of setting a threshold for the reduction procedure (N in eq. (3.3)), we try to estimate the factor C in eq. (3.11). In order to avoid divergences in the second derivatives, we modified the LJ potential in unphysical regions, i.e. for $r < 0.85$ we flattened the potential toward a constant value. We verified that our trajectories never visit such regions of the PES where the $r_{ij} < 0.9$ for any pair of atoms (i, j). With this choice of the potential, eq. (3.11) gives an

estimate $N = 27$. This is only an upper limit above which any contraction will be stable. Indeed, we verified that already for $N = 21$ the map is contractive. This allows us to solve iteratively the Fourier problem for the first 20 harmonics, and to treat the harmonics from $N + 1$ to $M = 320$ as a contraction.

The optimization of the first N harmonics was performed using conjugated residual method [21, 22], that is however tailored for sparse matrices, therefore not suited for a Fourier component optimization, thus affecting the efficiency of this step. After 5 steps of conjugate residual, the contraction procedure was started, and the fastest harmonics obtained from eq. (3.7) with a very fast iterative self consistent procedure.

Successive iterations of this procedure bring the total energy to an almost perfect conservation and the residual R_2 on the equations of motion to a value of $R \simeq 10^{-5}$ within a few steps (fig. 6.5). Since the conjugate residual is not an efficient procedure in this case, further improvement of the residual are rather slow (inset of fig. 6.5) and reaches the value $R_2 = 0.2 \cdot 10^{-5}$ in about 1000 iterations. To give an idea about efficiency, a single iteration of reduction with $N = 25$ and $M = 320$ has the cost of 10 Monte Carlo sweeps with 32 slices in the former annealing procedure (one sweep corresponds to an attempted move for each coordinate along the trajectory, i.e. 31×114 energy and force evaluations).

We show in figure 6.6 the potential and total energies of the final trajectories at $E_f = -110$ and $E_f = -150$. In figure 6.7 we show instead the fourfold and sixfold order parameter [23] along the path, for the first solution ($E_f = -150$) compared with the ones on the 32 slices path after the simulated annealing.

We must note that in order to improve further the residual R_2, we had to check periodically the assigned total energy, and to adjust it by a quantity within one percent. This behavior was probably due to the errors in the discretization and to the different definition of the kinetic energies in the cartesian and in the Fourier representation.

As a final check, we set as initial values the coordinates at halfway along the paths, and integrated back and forth the equations of motion using the Verlet algorithm. For both cases ($E_f = -150$ and $E_f = -110$) we were able to reach the initial and the final basin, obtaining a root mean square deviation of the Verlet trajectory from the optimized path of 0.06/atom/slice.

7. Conclusions. Two are the main results of this paper. First of all, Tonelli principle has been introduced and applied, for the first time to our knowledge, to realistic systems with several degrees of freedom. Maupertuis principle has many interesting features, because it provides a Riemannian metric and it allows for a local adaptivity of the time reparametrization. Otherwise Tonelli, with its stability properties and easy implementation, is an interesting alternative. *In our opinion the new introduced functional leads to a cleaner strategy because standard algorithms can be used even in situations where $\mathcal{M}_E$ shows problems.* We believe that in future works it would be worth to exploit its application to complex problems.

Moreover, a well defined reduction strategy has been presented which allows the successive inclusion of faster harmonics in the path. In this scheme the tail of the Fourier series is treated as a computationally convenient contraction. The procedure has been applied to examples of increasing complexity, including a 38 atom Lennard-Jones cluster, for which two trajectories discretized into 320 time slices, and two different preassigned total energies were found.

We are planning an improvement in the algorithms concerning the optimization of the slow harmonics, since the present conjugate residual method does not appear

to be efficient in Fourier representation.

We are aware that the initial value representation of molecular dynamics, although plagued by the well-known chaotic behavior [18], is computationally extremely convenient, and remains therefore the cornerstone of popular strategies such as path sampling [19]. However, the combination of the two concepts introduced here - Tonelli principle together with the finite reduction - should help in bridging the gap between initial value and two-point boundary representations in the field of rare events, not to mention the fact that the latter representations allows to obtain a detailed dynamical trajectory, at a given energy (even just above a barrier), joining two fixed points in the configuration space.

Acknowledgments. We thank G. F. Dell'Antonio, A. Gusev, A. Laio, D. Bai, R. Elber and M. Parrinello for insightful discussions. D. P. acknowledges CSCS (Swiss Center for Scientific Computing) for the use of computational resources.

REFERENCES

[1] L. Tonelli, *Sulle orbite periodiche*, Rend. R. Accad. dei Lincei, XXI-1 (1912) pp. 251–258 and 332–334.
[2] A. Ambrosetti and V. Coti Zelati, *Periodic solutions of singular Lagrangian systems*, Progress in Nonlinear Differential Equations and their Applications, Birkhäuser Boston, Inc., Boston, MA, pp. xii+157, 1993.
[3] G. F. Dell'Antonio, *Variational calculus and stability of periodic solutions of a class of Hamiltonian systems*, Special issue dedicated to Elliott H. Lieb. Rev. Math. Phys. 6 (1994), no. 5A, 1187–1232.
[4] H. Amann and E. Zehnder, *Periodic Solutions of Asymptotically Linear Hamiltonian Systems*, Manus. Math., 32 (1980), pp. 149–189.
[5] C. Conley and E. Zehnder, *The Birkhoff-Lewis fixed point theorem and a conjecture of V.I. Arnol'd*, Invent. Math., 73 (1983), pp. 33-49.
[6] L. Zanelli, P. Guiotto and F. Cardin, *Integral Representations of the Schrödinger propagator*, Reports on Mathematical Physics, to appear.
[7] R. P. Feynman and A. R. Hibbs, *Quantum mechanics and path integrals*, McGraw-Hill, New York, pp. xiv+365, 1965.
[8] J. D.Doll, *Monte Carlo Fourier Path Integral Methods in Chemical Dynamics*, J. Chem. Phys., 82 (1984), pp. 80.
[9] K. Mueller, *Reaction paths on multidimensional energy hypersurfaces*. Angew. Chem., 19 (1980), pp. 1-13.
[10] J. D. Doll, R. D. Coalson and D. L. Freeman, *Fourier path-integral Monte Carlo methods*: *Partial averaging*, Physical Review Letters, 55 1 (1985).
[11] A. E. Cho, J. D. Doll and D. L. Freeman, *The construction of double-ended classical trajectories*, Chemical Physics Letters, 229 3 (1994), pp. 218.
[12] R. E. Gillilan and K. R. Wilson, Shadowing, rare events, and rubber bands. A variational Verlet algorithm for molecular dynamics, J. Chem. Phys., 97 (1992), pp. 1757.
[13] R. Czerminski and R. Elber, *Reaction path study of conformational transitions in flexible systems*: *Applications to peptides*, Journal of Chemical Physics, 92 9 (1990), pp. 5580.
[14] R. Olender and R. Elber, *Calculation of classical trajectories with a very large time step*: *Formalism and numerical examples*, Journal of Chemical Physics, 105 20 (1996), pp. 9299.
[15] R. Elber, A. Ghosh and A. Cardenas, *Long Time Dynamics of Complex Systems*, Accounts of Chemical Research, 35 6 (2002), pp. 396.
[16] D. Bai and R. Elber, *Calculation of Point-to-Point Short-Time and Rare Trajectories with Boundary Value Formulation*, J. Chem. Theory Comput., 2 484 (2006).
[17] F. G. Wang and D. P. Landau, *Efficient, Multiple-Range Random Walk Algorithm to Calculate the Density of States*, Physical Review Letters, 86 10 (2001), pp. 2050.
[18] D. Passerone, *Computing the density of paths in complex systems*, Journal of Chemical Physics, 124 13 (2006).
[19] P. G. Bolhuis, C. Dellago and D. Chandler, *Sampling ensembles of deterministic transition pathways*, Faraday Discussions, 110 421 (1998).
[20] H. Jonsson, G. Mills and K. W. Jacobsen, in Computer Simulation of Rare Events and Dynamics of Classical and Quantum Condensed-Phase Systems – Classical and Quantum

Dynamics in Condensed Phase Simulations, edited by B. J. Berne, G. Ciccotti, and D. F. Coker, World Scientific, Singapore, pp. 385, 1998.

[21] D. Passerone, M. Ceccarelli and M. Parrinello, *A concerted variational strategy for investigating rare events*, Journal of Chemical Physics, 118 5 (2003), pp. 2025.

[22] Y. Saad *Iterative methods for sparse linear systems (2nd edition)*, SIAM, 2003.

[23] J. P. K. Doye, M. A. Miller and D. J. Wales, *The double-funnel energy landscape of the 38-atom Lennard-Jones cluster*, Journal of Chemical Physics, 110 14 (1999), pp. 6896.

[24] N. E. E, W. Q. Ren and E. Vanden-Eijnden, *String method for the study of rare events*, Physical Review B, 66 5 (2002), pp. 052301.